Novel Process for Diethylacetal Synthesis

Viviana M. T. M. Silva and Alírio E. Rodrigues
Laboratory of Separation and Reaction Engineering (LSRE), Dept. of Chemical Engineering, Faculty of Engineering, University of Porto, Rua Dr. Roberto Frias, 4200-465 Porto, Portugal

DOI 10.1002/aic.10531
Published online July 21, 2005 in Wiley InterScience (www.interscience.wiley.com).

This work presents the development of a novel process for the production of diethylacetal from the reaction between ethanol and acetaldehyde catalyzed by the acid resin Amberlyst® 15 using simulated moving-bed reactor (SMBR) technology. The methodology used combines modeling/simulation with laboratory- and pilot-scale experiments. The kinetic law of the reaction was measured from experiments in a batch catalytic reactor. The adsorption parameters were obtained from experiments performed in a fixed-bed adsorption column. Laboratory experiments in fixed-bed adsorptive reactors were performed and used to validate model and simulation tools. The SMBR technology was applied for diethylacetal production and separation with 87% purity and the acetaldehyde conversion was about 98%. The influence of feed composition, switching time, and mass-transfer resistance on the SMBR performance was analyzed by simulation. The reaction/separation region was determined using separation zone methodology. Simulated results show that high acetal purities can be achieved for 100% acetaldehyde conversion.
 AIChE J, 51: 2752–2768, 2005
Keywords: multifunctional reactors; process intensification; SMBR technology; diethylacetal synthesis; acid resin catalysis

Introduction

Acetaldehyde diethylacetal (herein called acetal) is an important raw material for fragrances and pharmaceuticals and is used in the flavoring of spirit drinks. In perfumery, acetal is used for the design of synthetic perfumes to increase the resistance to oxidation and therefore the lifetime of perfumes. Acetals have been under consideration as oxygenated additives to diesel fuel because they drastically reduce the emission of particles and NO_x while retaining or improving the cetane number and helping in the combustion of the final products, without decreasing the ignition quality.[1-4]

Diethylacetal production involves the reversible reaction of acetaldehyde and ethanol in acid medium according to: 2 ethanol (A) + acetaldehyde (B) ↔ acetal (C) + water (D)[5,6]; however, acetaldehyde could be replaced by vinyl ether, acetylene, or ethylene.[7] The advantage of using ethanol and acetaldehyde as reactants is that ethanol is produced from renewable sources (mainly from the sugarcane industry) and acetaldehyde could be produced from dehydrogenation of ethanol or direct ethylene oxidation.

Traditionally, the reaction is catalyzed by mineral or carboxylic acids.[8] The disadvantage of using soluble catalysts is that they must be neutralized after the reaction and separated from the product. Therefore, heterogeneous catalysts as ion-exchange resins (acid type) or zeolites are used, which have the advantages of being easily separated from the reaction product and having a long lifetime. Acid resins are interesting because they serve as catalysts for the acetalization reaction and selective adsorbents for the species involved in the process. Ion-exchange resins conventionally used to catalyze etherification and esterification reactions[9,10] can be used, such as Dowex 50 (Dow Chemical, Midland, MI), Amberlite® IR120, Amberlyst® A15 and A36 (Rohm and Haas, Philadelphia, PA), and Lewatit® (Bayer AG, Leverkusen, Germany).

To obtain acceptable acetal yield, the reaction equilibrium must be displaced in the direction of acetal synthesis. Several methods are used to achieve that objective:

(1) To use a large excess of one of the reactants, generally

V. M. T. M. Silva is on temporary leave from School of Technology and Management, Bragança Polytechnic Institute, Campus de Santa Polónia, Apartado 1134, 5301-857 Bragança, Portugal.
Correspondence concerning this article should be addressed to A. E. Rodrigues at arodrig@fe.up.pt.

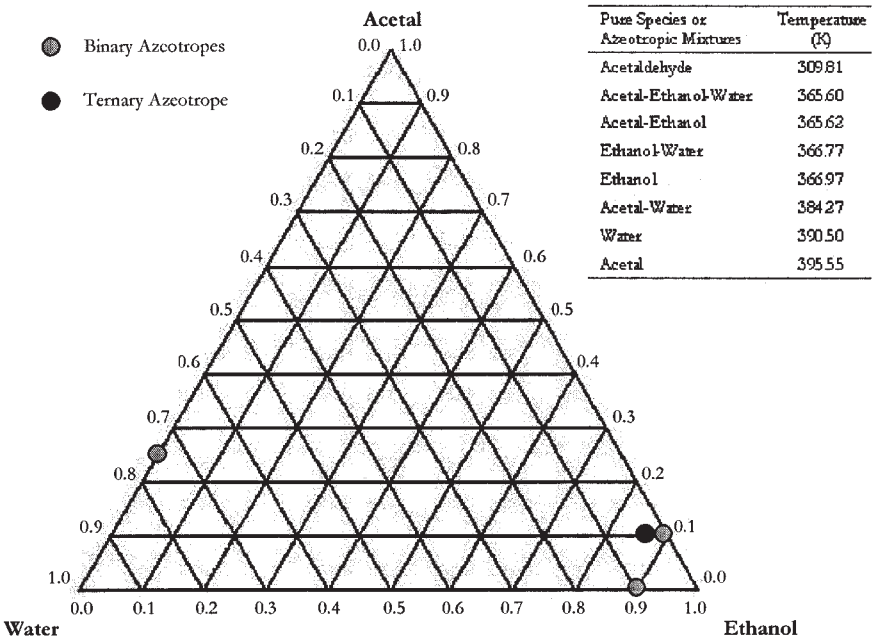

Pure Species or Azeotropic Mixtures	Temperature (K)
Acetaldehyde	309.81
Acetal-Ethanol-Water	365.60
Acetal-Ethanol	365.62
Ethanol-Water	366.77
Ethanol	366.97
Acetal-Water	384.27
Water	390.50
Acetal	395.55

Figure 1. Azeotropes for the ternary system acetal–ethanol–water, and boiling points for pure species and azeotropic mixtures at 1.8 atm.[55]

the alcohol, which then requires elimination of that excess in a step of purification of the desired product.

(2) To eliminate water by azeotropic distillation between a solvent and water, the solvent and water must be partially miscible and the boiling points of the different constituents in the reaction medium must be compatible with that azeotrope.

(3) To use reactive separations (such as reactive distillation, simulated moving-bed reactor, pervaporation membrane reactor, etc.) to remove the products from the reaction medium.

The conventional manufacturing processes use energy-intensive distillation steps. The acetal–ethanol–water subsystem exhibits three binary azeotropes and one ternary azeotrope, as shown in Figure 1. The complexity of the vapor–liquid and liquid–liquid equilibrium makes the design and the synthesis of separation sequences a difficult task.

Innovative reactor configurations and choice of operating conditions can improve the selectivity of the desired product and reduce the cost associated with the separation step. In recent years there has been increased interest in the area of reactive separations, where reaction and separation are combined in a single step. Reactive separations offer the following advantages: increased conversion of reactants beyond thermodynamic limit; improved yield of desired products; reduced requirements for external energy supply or cooling capacity; and reduced capital costs by process intensification. The advantages of coupling chemical reaction and separation have been exploited since 1921[11] for methyl acetate production with reactive distillation (RD) process[12] and have been applied in the petrochemical industry. RD technology is also being applied for (1) production of oxygenates such as methyl *tert*-butyl ether (MTBE),[13,14] ethyl *tert*-butyl ether (ETBE),[15] or tertiary amyl methyl ether (TAME)[16] and (2) acetalization of formaldehyde with methanol.[17] However, there are constraints and difficulties in RD implementation, mainly volatility constraints. It is necessary that both products have different boiling points to ensure the separation; therefore, the production of diethylacetal using RD technology is not feasible, given the close boiling points of acetal and water.

For the last 30 years, the concept of chromatographic reactors has been extended to continuous processes to benefit from those features as enhanced productivity and decreased solvent consumption. Among the continuous chromatography processes, the simulated moving bed (SMB) technology has provided one of the most convenient solutions for separations in pharmaceutical and fine chemical industries. The combination of the chemical or biochemical reaction with SMB has recently been the subject of considerable attention in the scientific research. This integrated reaction–separation technology is called *simulated moving-bed reactor* (SMBR) technology.

The SMBR unit and principle of its operation is presented in Figure 2, where a reaction of type $2A + B \leftrightarrow C + D$ is considered. The SMBR consists of a set of interconnected columns packed with a solid, which acts as both adsorbent and catalyst. There are two inlet streams (feed and desorbent) and two outlet streams (extract and raffinate). The reactants A and B are used as feed; the component A is also used as desorbent;

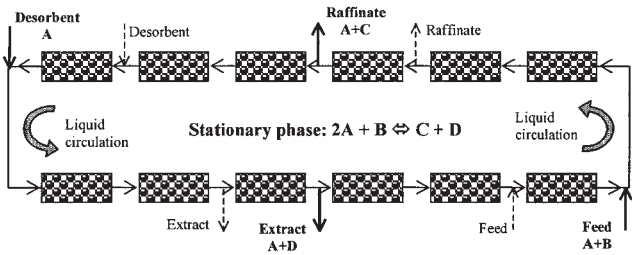

Figure 2. Simulated moving-bed reactor.

Dashed lines stand for the position of streams in the last period before the present one (continuous lines).

the more adsorbed product D and the less adsorbed product C are collected in the extract and the raffinate, respectively. At regular time intervals, called switching time period, the inlet and outlet ports are switched for one bed distance in direction of the fluid flow. A cycle is completed when the number of switches is an integer multiple of the number of columns. In this way, the countercurrent motion of the solid is simulated with a velocity equal to the length of a column divided by the switching time. According to the position of the inlet and outlet stream the unit can be divided in four sections. In section I, placed between the desorbent and extract nodes, the adsorbent is regenerated by desorption of the more strongly adsorbed product (D) from the solid. In section II (between the extract and feed node) and section III (between the feed and raffinate node) the reaction is taking place and products (C and D) are formed. The more strongly adsorbed product D is adsorbed and transported with the solid phase to the extract port. The less strongly adsorbed product (C) is desorbed and transported with the liquid in the direction of the raffinate port. In section IV, placed between the raffinate and desorbent node, the eluent is regenerated before being recycled to section I.

Because the acetalization is controlled by chemical equilibrium, the removal of the reaction products leads to conversion of reactants above the equilibrium limit. The production and separation of diethylacetal in the SMBR seems to be a feasible process. Although SMBR technology allows 100% of conversion with 100% of recovery of the desired product (acetal), a further step is necessary to separate the product from the raffinate mixture. Nevertheless, the complexity of the separation steps is reduced: two binary streams (ethanol/acetal and ethanol/water) have to be separated instead of the quaternary mixture produced in a conventional reactor. The use of a pervaporation membrane process to separate ethanol from acetal[18,19] and ethanol from water[20,21] seems be feasible and will avoid formation of azeotropes. Moreover, for some applications there is no need to carry out ethanol/acetal separation.

The first gas-phase applications of the SMBR were the hydrogenation of 1,3,5-trimethylbenzene[22] and the oxidative coupling of methane.[23] Several liquid-phase SMBR applications are found in the literature. Examples of biochemical reactions are the isomerization of glucose with glucose isomerase,[24-27] the inversion of sucrose by action of invertase,[28,29] and the production of lactosucrose by action of b-fructofuranosidase.[30] Examples of reversible chemical reactions catalyzed by ion-exchange resins are the esterification of acetic acid with b-phenetyl alcohol,[31] the ethyl acetate synthesis on Amberlyst® 15,[9,32] the synthesis of bisphenol A from acetone and phenol,[33] esterification of acetic acid with methanol,[34] and synthesis of MTBE.[35] Another example is the dismutation of toluene into benzene and xylenes.[36] The design and optimization of SMBR to carry out simultaneous and continuous reaction and separation are of importance to analyze the process feasibility at industrial scale.[32,37-41]

The objective of the study reported herein is the development of a novel process for diethylacetal synthesis from ethanol and acetaldehyde catalyzed by the acid resin Amberlyst® 15 using SMBR technology. The methodology used is as follows:

(1) The measurement of the kinetic law of reaction from batch catalytic reactor experiments.

(2) The measurement of adsorption data for nonreactive binary mixtures in fixed-bed columns packed with the adsorbent/catalyst particles of Amberlyst® 15.

(3) The synthesis of diethylacetal in a fixed-bed adsorptive reactor to test and validate the mathematical model and simulation tools.

(4) The development of an SMBR simulator that allows the study of the influence of feed composition, mass transfer, and switching time on SMBR performance.

(5) The synthesis of diethylacetal in an SMBR pilot unit Licosep® 12-26 (Novasep, Vandoeuvre-les-Nancy, France) and assessment of the performance predicted by the simulator.

Kinetic Studies in Batch Catalytic Reactor

The synthesis of diethylacetal was studied in a batch reactor by reacting ethanol and acetaldehyde in the liquid phase, using two acid resins as catalyst: Amberlyst® 18 (A18)[42] and Amberlyst® 15 (A15).[43]

The reaction equilibrium constant was determined experimentally in the temperature range 20–60 °C at 1.0 MPa

$$\ln K_{eq} = 1270/T(\mathrm{K}) - 3.07 \tag{1}$$

Kinetic experiments were carried out in the temperature range 16–26 °C at 0.6 MPa, with Amberlyst® 18. A two-parameter model based on a Langmuir–Hinshelwood rate expression, using activities, can describe the experimental kinetic results. The proposed kinetic law is

$$\Re = k_c \frac{a_A a_B - \dfrac{a_C a_D}{K_{eq} a_A}}{(1 + K_D a_D)^2} \tag{2}$$

and the parameters are

$$k_C\,(\mathrm{mol\ g^{-1}\ min^{-1}}) = 3.3 \times 10^{11} \exp\left[\frac{-7824}{T\,(\mathrm{K})}\right] \tag{3}$$

$$K_D = 6.4 \times 10^5 \exp\left[\frac{-4003}{T\,(\mathrm{K})}\right] \tag{4}$$

The activity coefficients of compounds were computed by the UNIFAC method.[44] The parameters needed for its use (relative molecular volume and surface area of pure species and the interaction parameters) are presented in Tables 1 and 2.

The resins Amberlyst® 18 and 15 have similar properties, as shown in Table 3. To verify whether the rate law obtained with Amberlyst® 18 catalyst is applicable to the Amberlyst® 15 catalyst, two kinetic experiments with Amberlyst® 15 were carried out in a batch reactor (see Figure 3). The simulations were performed with the pore diffusion model, using the kinetic parameters obtained with Amberlyst® 18 catalyst. The simulated curves predicted reasonably well the Amberlyst® 15 kinetic experimental results and so the kinetic parameters obtained with Amberlyst® 18 could be used to describe the adsorptive fixed-bed reactor packed with Amberlyst® 15.

Table 1. Relative Molecular Volume and Surface Area of Pure Species Parameters[53]

Molecule (i)	Group Identification: Name	No. Main	No. Sec.	$\zeta_k^{(i)}$	R_k	Q_k
1: Ethanol	CH_3	1	1	1	0.9011	0.848
	CH_2	1	2	1	0.6744	0.540
	OH	5	15	1	1.0000	1.200
2: Acetaldehyde	CH_3	1	1	1	0.9011	0.848
	CHO	10	21	1	0.9980	0.948
3: Acetal	CH_3	1	1	3	0.9011	0.848
	CH	1	3	1	0.4469	0.228
	CH_2O	13	26	2	0.9183	0.780
4: Water	H_2O	7	17	1	0.9200	1.400

Adsorption Data from a Chromatographic Column

The adsorption data were obtained for Amberlyst® 15 by performing dynamic binary experiments at 15°C. The breakthrough curves of ethanol, acetal, and water were measured in the absence of reaction. The resin was saturated with a certain component A and then the feed concentration of component B was changed stepwise. The adsorption parameters were optimized by minimizing the difference between experimental and theoretical number of moles adsorbed/desorbed for all adsorption experiments. Two columns were tested: one at pilot scale with 86 cm length and 2.2 cm diameter and the other at laboratory scale with 23 cm length and 2.6 cm diameter. The conditions of the binary adsorption experiments are summarized in Table 4.

The multicomponent Langmuir adsorption model was considered. The optimization of the adsorbed/desorbed number of moles of each component was done for all experiments, leading to the adsorption parameters shown in Table 5. For these values of adsorption parameters the error percentage between the number of moles adsorbed/desorbed for each component, in all experiments, was $1<2\%$ for the experiments carried out at 15 °C and $<5\%$ for the experiments performed at 10°C, as shown in Table 6.

The comparison between experimental and simulated results is presented in Figure 4. The mass balance was checked for a set of experiments where the column was initially saturated with pure ethanol, and ethanol was replaced by acetal or water, and finally the column was regenerated with pure ethanol. For example, considering runs 1, 2, and 3, the total amount of ethanol desorbed during runs 1 and 2 was 2.672 moles, which were replaced with 1.098 moles of acetal. During the regeneration step, 2.679 moles of ethanol were needed to displace 1.106 moles of acetal, leading to an error of $<1\%$.

Table 2. Interaction Parameters[54]

$a_{m,n}$	1	5	7	10	13
1	0	986.5	1318	677	251.5
5	156.4	0	353.5	−203.6	28.06
7	300	−229.1	0	−116	540.5
10	505.7	529	480.8	0	304.1
13	83.36	237.7	−314.7	−7.838	0

Table 3. Physical and Chemical Properties for Amberlyst® 18 and Amberlyst® 15*

Property	Amberlyst® 18	Amberlyst® 15
Moisture content	51–54%	52–57%
Shipping weight	790 g/L	770 g/L
Particle size	0.2–1.2 mm	0.3–1.2 mm
Concentration of acid sites	1.8 meq/mL	1.7 meq/mL
Surface area	30 m^2/g	45 m^2/g
Porosity	0.63 mL/g	—
Average pore diameter	43 nm	24 nm

*Supplier information.

Synthesis of Diethylacetal in a Fixed-Bed Adsorptive Reactor

The diethylacetal synthesis was performed in a fixed-bed adsorptive reactor packed with Amberlyst® 15. In a typical reaction experiment, a mixture of ethanol and acetaldehyde is continuously fed to the chromatographic reactor initially saturated with ethanol. Because the feed mixture is less dense than ethanol, the direction flow adopted was from the top to bottom of the column. In the regeneration experiment, ethanol was used as desorbent and the top-down flow was adopted because the reaction mixture present within the column is heavier than pure ethanol.

The dynamic behavior of a fixed bed for the synthesis of diethylacetal was predicted by a mathematical model for the adsorptive reactor, which considers axial dispersion, mass-transfer resistances, constant temperature, multicomponent

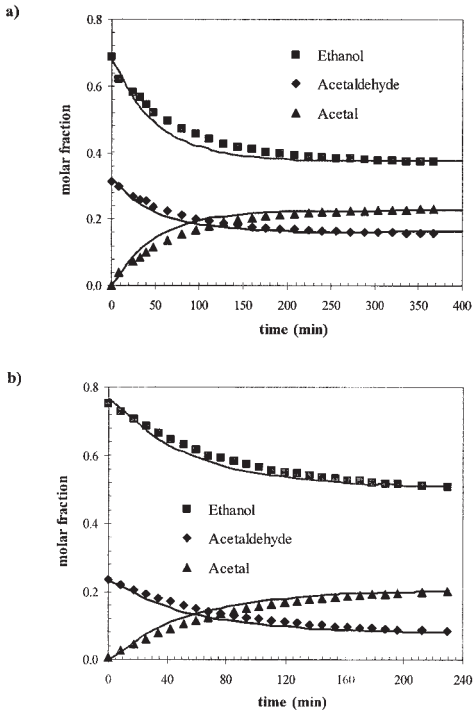

Figure 3. Kinetic experiments performed in a batch reactor with Amberlyst® 15.

$T = 15$°C, $P = 6$ atm, $d_p = 267$ μm, $w_{cat} = 0.5$ g, Experimental conditions: (a) $C_{A0} = 11.97$ mol/L and $C_{B0} = 5.45$ mol/L; (b) $C_{A0} = 13.36$ mol/L and $C_{B0} = 4.01$ mol/L.

Table 4. Experimental Conditions of the Adsorption Experiments*

Factor	Run 1	2	3	4	5	6	7	8	9
Adsorption	acetal	acetal	ethanol	water	water	ethanol	acetal	acetal	ethanol
Desorption	ethanol	ethanol	acetal	ethanol	ethanol	water	ethanol	ethanol	acetal
L_{col} (cm)	86	86	86	86	86	86	23	23	23
Q (mL/min)	2.6	3.7	3.2	8.0	9.2	9.0	12.0	12.7	12.7
T (°C)	15.0	15.0	15.0	15.0	15.0	15.0	10.0	10.0	10.0
$C_{0,A}$ (mol/L)	17.13	9.38	5.09	17.17	15.69	12.89	17.16	8.26	3.13
$C_{0,B}$ (mol/L)	0.00	3.21	4.98	0.26	5.04	14.05	0.00	3.64	5.75
$C_{f,A}$ (mol/L)	9.35	5.08	17.15	15.66	12.94	17.10	8.24	3.12	17.15
$C_{f,B}$ (mol/L)	3.21	4.98	0.00	5.13	13.91	0.49	3.66	5.75	0.00

*Component A: ethanol; component B: acetal or water.

Langmuir adsorption isotherms, and reaction rate expressed in terms of activities.[45] The theoretical model considers two mass-transfer resistances in series: the external film and the diffusion inside the pores. The internal mass-transfer coefficients were estimated by the linear driving force Glueckauf approximation[46] and the Wilson–Geankoplis correlation[47] was used to estimate the external mass-transfer coefficients. Model equations were solved by orthogonal collocation by finite elements, using the measured model parameters. The model was validated by comparison with the experimental results obtained for the production and regeneration steps. The model is able to predict the response of adsorptive reactors with different lengths for a wide range of initial/feed compositions. The model developed as well as the reaction and adsorption data for Amberlyst® 15 will be applied in the analysis of the SMBR.

Figure 5 shows the concentration histories for the production and regeneration steps for a typical experiment performed in a laboratory-scale column, packed with Amberlyst® 15. To ensure that the behavior of the fixed-bed adsorptive reactor is well described for different range of compositions, a kinetic experiment was performed in a pilot-scale column packed with A15, initially saturated with a mixture of ethanol and water. Then, a mixture containing ethanol, acetaldehyde, and water was fed to the column until the equilibrium has been reached (Figure 6a) and the regeneration of the resin was performed with pure ethanol (Figure 6b). All adsorptive and reactive concentration fronts are well predicted by the proposed model.

The Simulated Moving-Bed Reactor

Experimental apparatus

All SMBR experiments were performed in a pilot unit Licosep® 12-26 by Novasep. Twelve columns of Superformance SP 230 × 26 (length × ID, mm), by Götec Labortechnik (Mühltal, Germany), packed with the acid resin Amberlyst® 15 (Rohm and Haas) were connected to the SMBR pilot unit. Each column is jacketed to ensure temperature control and the jackets are connected to one another by silicone hoses and to a thermostat bath (Lauda GmbH, Lauda-Königshofen, Germany). The operating temperature was 10°C. Between every two columns there is a four-port valve actuated by the control system. When required, the valves allow either pumping of feed/eluent into the system or withdrawal of extract/raffinate streams. Each of the inlet (feed and eluent) and outlet (extract and raffinate) streams is pumped by means of HPLC pumps. The recycling pump is a positive-displacement three-head membrane pump (Milton Roy, Pont St. Pierre, France), which may deliver flow rates as low as 20 mL/min up to 120 mL/min. The other flows (desorbent, extract, feed, and raffinate) are controlled by four pumps (models L-6000 and L-6200; Merck–Hitachi, Darmstadt, Germany), connected to computer by an RS-232. The maximum flow rate in the desorbed and extract pumps is 30 mL/min, whereas in the feed and raffinate pumps the flow rate is 10 mL/min. The maximum allowable pressure is 60 bar. Between the twelfth and the first columns there is a six-port valve, used to collect samples for internal concentration profile measurements. Figure 7 shows a side view of the pilot unit, where six columns are placed. The other six columns used in most experiments are placed on the other side. The equipment has its own process control software, which is able to accomplish the following tasks:

- Switch the inlet and outlet streams at regular time intervals (as assigned by the user) by opening and closing on–off pneumatic valves.
- Keep steady and constant section flow rates as assigned.
- Keep suction pressure at the recycling pump around a set point assigned by the user (usually 1.5 bar).

Each of the twelve columns was subjected to pulse experiments of tracer (blue dextran solution) to verify the homogeneity of packing and determine bed porosity under the flow rates of 15–40 mL/min. The bed porosity and the Peclet (Pe) number were calculated from the stoichiometric time and the second moment of the obtained experimental pulse curves. An average Peclet number of 300 was obtained for the range of flow rates to be used in the fixed-bed experiments. The mean value obtained for porosity was 0.40. It was verified that the axial mixing did not vary significantly from column to column and in the flow range studied. The columns were all assumed to be homogeneously packed with axial mixing accounted for by assigning Pe = 300 in the range of flow rates to be used in the SMB. The characteristics of the SMB columns used in the simulations are presented in Table 7.

Table 5. Adsorption Equilibrium Parameters for Langmuir Isotherms over A15

Component	Q_{ads} (mol/L_{res})	K (mol/L)
Ethanol	14.3	1.43
Acetaldehyde	20.1	1.58
Acetal	11.45	0.09
Water	44.7	2.01

Table 6. Experimental and Theoretical Values for the Number of Moles Adsorbed/Desorbed*

Parameter	Run 1	2	3	4	5	6	7	8	9
$n_{exp,A}$ (mol)	−1.664	−1.008	2.679	−0.802	−1.035	1.834	−0.709	−0.456	1.159
$n_{exp,B}$ (mol)	0.683	0.415	−1.106	2.587	3.338	−5.918	0.291	0.184	−0.474
$n_{theo,A}$ (mol)	−1.664	−1.020	2.679	−0.802	−1.054	1.814	−0.686	−0.476	1.158
$n_{theo,B}$ (mol)	0.683	0.415	−1.097	2.587	3.400	−5.849	0.280	0.192	−0.470
Δn_A (%)	0.02	1.17	0.01	0.00	1.84	1.09	3.20	4.32	0.07
Δn_B (%)	0.05	0.00	0.75	0.00	1.83	1.16	3.94	4.21	0.90

*Component A: ethanol; component B: acetal or water.

Mathematical model

The SMBR modeling strategy is more precise than the true moving-bed reactor (TMBR) model because it depicts the actual physical equipment operation. It allows the visualization of the axial movement of concentration profiles and the variations in extract and raffinate concentrations within a period. However, it demands considerably higher computational effort than the TMBR strategy, especially when a great many columns are involved. For this case the cyclic behavior of the SMBR can be predicted from the steady-state model of the TMBR with good accuracy, as will be shown below. Therefore, the mathematical model used to describe the SMBR performance is based on the TMBR strategy considering axial dispersion flow for the bulk fluid phase, plug flow for the solid phase, linear driving force (LDF) for the particle mass transfer rate, and multicomponent adsorption equilibria. Constant column length and packing porosity are also assumed. The model equations are as follows.

Bulk Fluid Mass Balance to Component i at Section j

$$\frac{\partial C(i,j,z,t)}{\partial t} + \frac{(1-\varepsilon)}{\varepsilon}\frac{3}{r_p}K_L(i,j,z,t)[C(i,j,z,t) - \bar{C}_p(i,j,z,t)] = D_{ax}(j)\frac{\partial^2 C(i,j,z,t)}{\partial z^2} - u(j)\frac{\partial C(i,j,z,t)}{\partial z} \quad (5)$$

where C and $\bar{C}_p$ are the bulk and average particle concentrations at fluid phase of species i in section j of the TMBR, respectively; K_L is the global mass-transfer coefficient of component i; ε is the bulk porosity; t is the time variable; z is the

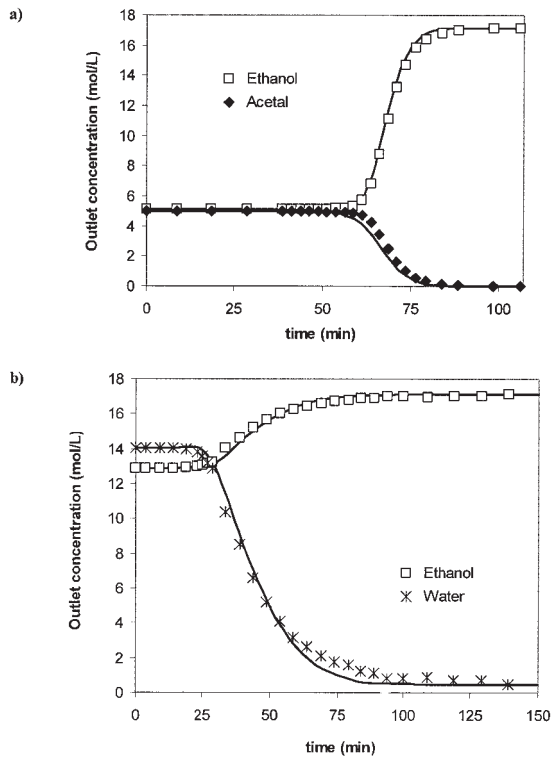

Figure 4. Breakthrough experiments performed with binary mixtures in a column packed with Amberlyst® 15 with 85 cm of length.

(a) Ethanol displacing acetal (run 3). (b) Ethanol displacing water (run 6).

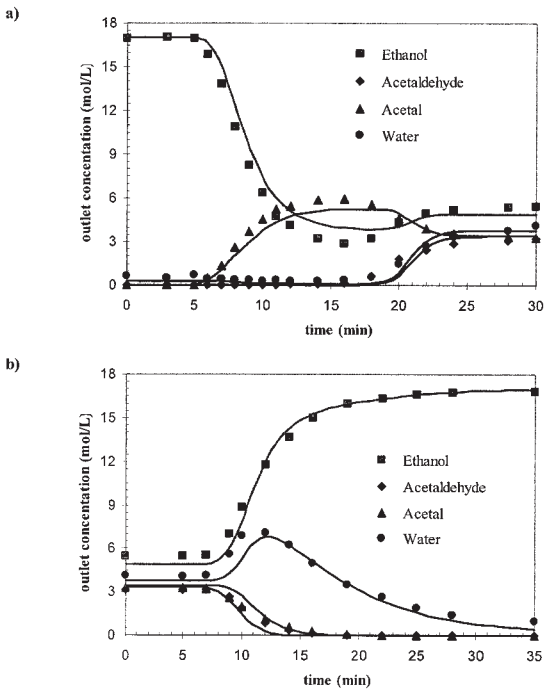

Figure 5. Concentration histories in a fixed bed adsorptive reactor packed with Amberlyst® 15 with particle diameter d_p = 800 μm and 23 cm of length, at 10°C.

Experimental conditions: (a) Production step: column initially saturated with ethanol and then fed with ethanol and acetaldehyde (C_{A0} = 11.7 mol/L and C_{B0} = 6.8 mol/L) at Q = 9.5 mL/min. (b) Regeneration step with pure ethanol at Q = 10.2 mL/min.

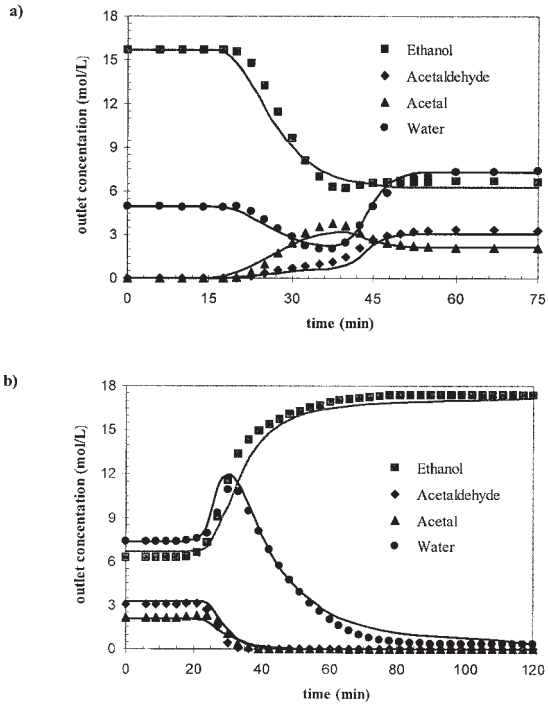

Figure 6. Concentration histories in a fixed-bed adsorptive reactor packed with Amberlyst® 15 with particle diameter d_p = 700 μm and 86 cm of length, at 15°C.

Experimental conditions: (a) Production step: column initially saturated with a mixture of ethanol/water and then fed with a mixture of ethanol/acetaldehyde/water (C_{A0} = 10.6 mol/L, C_{B0} = 5.2 mol/L, and C_{D0} = 5.2 mol/L) at Q = 9.2 mL/min. (b) Regeneration step with pure ethanol at Q = 9.0 mL/min.

axial coordinate; D_{ax} and u are the axial dispersion coefficient and the interstitial velocity at section j, respectively; and r_p is the particle diameter.

Pellet Mass Balance to Component i at Section j

$$U_s\left[\varepsilon_p \frac{\partial \bar{C}_p(i,j,z,t)}{\partial z} + (1-\varepsilon_p)\frac{\partial q(i,j,z,t)}{\partial z}\right] + \frac{3}{r_p}K_L(i,j,z,t)[C(i,j,z,t) - \bar{C}_p(i,j,z,t)] = \varepsilon_p \frac{\partial \bar{C}_p(i,j,z,t)}{\partial t} + (1-\varepsilon_p)\frac{\partial q(i,j,z,t)}{\partial t} - \nu(i)\rho_p\eta\Re[C(i,j,z,t)] \quad (6)$$

where q is the adsorbed phase concentration of species i in section j in equilibrium with $\bar{C}_p$, U_s is the solid interstitial velocity, ε_p is the particle porosity, ν is the stoichiometric coefficient of component i, ρ_p is the particle density, η is the effectiveness factor of the catalyst, and $\Re$ is the rate of the chemical reaction relative to the bulk liquid phase. The effectiveness factor is assumed to be constant. This assumption is acceptable because no significant variations were observed along the transient state of kinetic experiments performed in the batch reactor.[43] An effectiveness factor of 0.34 was used for the simulations of the SMBR experiments, corresponding to the experimental conditions: T = 10 °C and d_p = 800 μm.

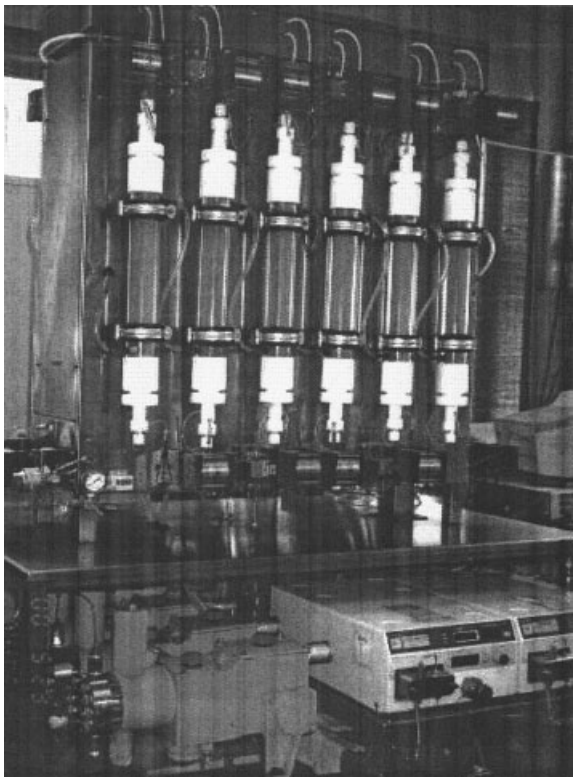

Figure 7. SMB pilot unit Licosep® 12-26 at LSRE.

Initial and Danckwerts Boundary Conditions

$$t = 0 \qquad C(i,j,z,0) = \bar{C}_p(i,j,z,0) = C_0(i) \quad (7)$$

$$z = 0 \qquad C(i,j,0,t) - \frac{D_{ax}(j)}{u(j)}\left.\frac{\partial C(i,j,z,t)}{\partial z}\right|_{z=0} = C_{in}(i,j,t) \quad (8)$$

$$z = L_j \qquad \left.\frac{\partial C(i,j,z,t)}{\partial z}\right|_{z=L_j} = 0 \quad (9)$$

where subscripts *in* and 0 refer to the section inlet and initial state, respectively.

Table 7. Characteristics of the Simulated Moving-Bed Columns

Length (L)	23 cm
Internal diameter	2.6 cm
Radius of the particle (r_p)	400 μm
External void fraction (ε)	0.40
Internal void fraction (ε_p)	0.40
Peclet number	300
Bulk density (ρ_b)	390 kg/m^3

Table 8. Operating Conditions and Experimental/Simulated Performance Parameters of the SMBR Unit

Run 1	Run 2	Run 3
$t^* = 3.50$ min	$t^* = 3.75$ min	$t^* = 4.00$ min
$Q_D = 23.5$ mL/min	$Q_D = 22.7$ mL/min	$Q_D = 24.0$ mL/min
$Q_4 = 20.5$ mL/min	$Q_4 = 21.3$ mL/min	$Q_4 = 20.0$ mL/min
$C_{C,R} = 2.37$ mol/L	$C_{C,R} = 3.00$ mol/L	$C_{C,R} = 2.90$ mol/L
$PUR = 79.1\ (87.3)$ %	$PUR = 84.1\ (90.2)$ %	$PUR = 87.2\ (90.0)$
$PUX = 97.8\ (95.2)$ %	$PUX = 95.2\ (97.4)$ %	$PUX = 96.1\ (98.3)$
$PR = 3.66\ (4.21)$ kg L^{-1} day^{-1}	$PR = 4.65\ (4.61)$ kg L^{-1} day^{-1}	$PR = 4.48\ (4.05)$ kg L^{-1} day^{-1}
$DC = 9.81\ (8.53)$ L/kg	$DC = 7.45\ (7.50)$ L/kg	$DC = 8.20\ (9.06)$ L/kg
$X = 97.7\ (98.6)$ %	$X = 98.1\ (98.7)$ %	$X = 98.2\ (99.0)$ %

Multicomponent Adsorption Equilibrium Isotherm

$$q(i, j, z, t) = \frac{Q_{ads}(i)\, K(i) \bar{C}_p(i, j, z, t)}{1 + \sum_{l=1}^{n} K(l) \bar{C}_p(l, j, z, t)} \tag{10}$$

where Q_{ads} and K represent the total molar capacity per unit volume of resin and the equilibrium constant, respectively.

Mass Balances at the Nodes of the Inlet and Outlet Lines of the TMBR

- Eluent node

$$C(i, I, 0, t) = \frac{u_{\mathrm{IV}}}{u_{\mathrm{I}}} C(i, \mathrm{IV}, L_{\mathrm{IV}}, t) + \frac{u_D}{u_{\mathrm{I}}} C_D(i) \tag{11}$$

- Extract node

$$C(i, \mathrm{II}, 0, t) = C(i, \mathrm{I}, L_{\mathrm{I}}, t) \tag{12}$$

- Feed node

$$C(i, \mathrm{III}, 0, t) = \frac{u_{\mathrm{II}}}{u_{\mathrm{III}}} C(i, \mathrm{II}, L_{\mathrm{II}}, t) + \frac{u_F}{u_{\mathrm{III}}} C_F(i) \tag{13}$$

- Raffinate node

$$C(i, \mathrm{IV}, 0, t) = C(i, \mathrm{III}, L_{\mathrm{III}}, t) \tag{14}$$

with the relations between fluid velocities in the four zones of the TMBR:

$$u_{\mathrm{I}} = u_{\mathrm{IV}} + u_D \qquad u_{\mathrm{II}} = u_{\mathrm{I}} - u_X \qquad u_{\mathrm{III}} = u_{\mathrm{II}} + u_F \qquad u_{\mathrm{IV}} = u_{\mathrm{III}} - u_R \tag{15}$$

where u_{I}, u_{II}, u_{III}, and u_{IV} are the fluid velocities at sections I, II, III, and IV, respectively. The subscripts D, X, F, and R refer to the desorbent, extract, feed, and raffinate streams, respectively.

The SMBR model is similar to the TMBR model with the following differences:

- The SMBR mass balances are written for each column instead of each section as in the TMBR.
- The pellet mass balance for the SMBR model does not include the term relative to the solid velocity.
- The liquid interstitial velocities in the SMBR are higher than those in the TMBR model: $u^{\mathrm{SMBR}} = u^{\mathrm{TMBR}} + U_s$, where the solid interstitial velocity of the TMBR model is related with the switching time t^* of the SMBR model: $U_s = L/t^*$.
- The boundary at L position for each column which is not in node position is: $C(i, j, L_c, t) = C(i, j + 1, 0, t)$

SMBR performance criteria

The SMBR process performance will be evaluated accordingly the following criteria:

Raffinate Purity (%)

$$PUR = \frac{C_{C,R}}{C_{B,R} + C_{C,R} + C_{D,R}} \times 100 \tag{16}$$

Extract Purity (%)

$$PUX = \frac{C_{D,X}}{C_{B,X} + C_{C,X} + C_{D,X}} \times 100 \tag{17}$$

Acetaldehyde Conversion (%)

$$X = 1 - \frac{Q_X C_{B,X} + Q_R C_{B,R}}{Q_F C_{B,F}} \tag{18}$$

Raffinate Productivity ($kg_{acetal}\ L^{-1}_{adsorbent}\ day^{-1}$)

$$PR = \frac{Q_R C_{C,R}}{(1 - \varepsilon) V_{unit}} \tag{19}$$

Desorbent Consumption ($L_{ethanol}/kg_{acetal}$)

$$DC = \frac{[Q_D C_{A,D} + Q_F (C_{A,F} - 2X C_{B,F})] V_{ml,A}}{Q_R C_{C,R}} \tag{20}$$

The productivity is defined just for the raffinate stream because acetal is the desired product. The definition of desorbent consumption takes into consideration just the amount of ethanol that is used as desorbent, and not the ethanol consumed in the reaction.

Model equations were numerically solved by using the gPROMS (*g*eneral *PRO*cess *M*odeling *S*ystem)[48] software package for modeling and simulation of processes with both discrete and continuous as well as lumped and distributed characteristics. The mathematical model involves a system of

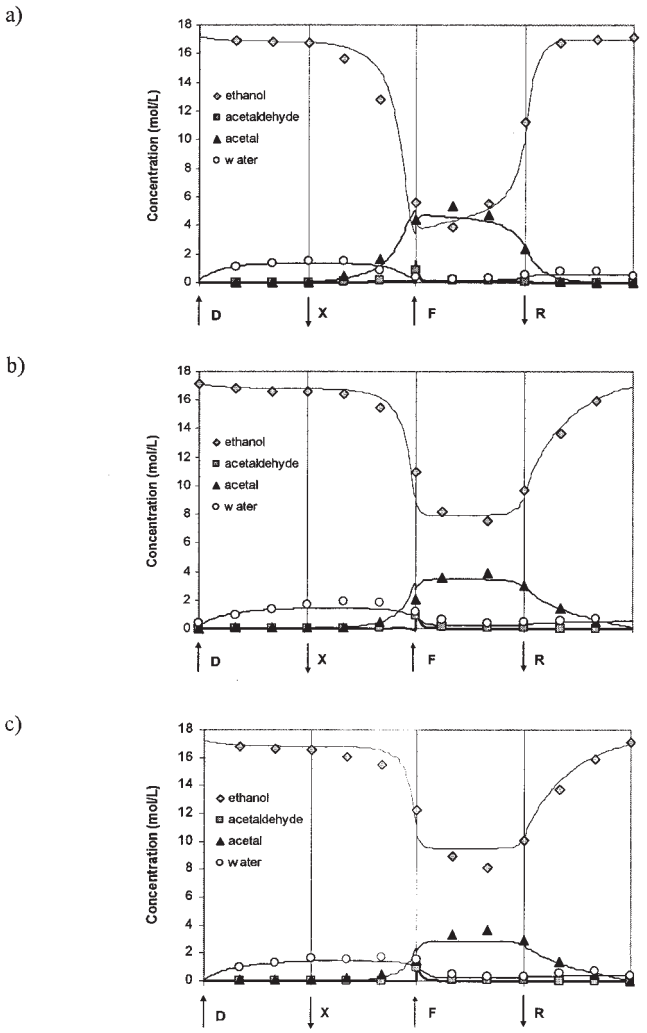

Figure 8. Experimental concentration profiles in a SMBR at the middle of a switching time at cyclic steady-state (10th cycle) and simulated curves.

(a) Run 1; (b) run 2; (c) run 3.

partial and algebraic equations (PDAEs). Third-order orthogonal collocation method in finite elements (OCFEM) was used in the discretization of axial domain. Twenty equal elements per section with two collocation points in each element were used. The system of ordinary differential and algebraic equation (ODAEs) was integrated over time using the DASOLV integrator implement in gPROMS. A tolerance value of 10^{-5} was fixed for all simulations. In the case of the SMBR model six finite elements per column with two collocation points in each element were used.

Results and Discussion

Experimental results

The SMBR experiments were performed under conditions of incomplete adsorbent regeneration in section I because of equipment limitations. The recycle pump was operated at the minimum flow rate (20 mL/min). Pure ethanol was used as desorbent.

Three experiments of diethylacetal synthesis were carried out at 10°C in the SMBR unit, with three columns per section. The feed composition was a mixture of ethanol and acetaldehyde, with 51% acetaldehyde molar fraction ($C_{A,F}$ = 8.57 mol/L, $C_{B,F}$ = 8.96 mol/L). The flow rates of feed and raffinate streams were Q_F = 3.0 mL/min and Q_R = 8.0 mL/min. The other experimental conditions and the SMBR experimental and simulated (inside brackets) performance criteria are presented in Table 8. By increasing the switching time from 3.5 to 4.0 min, the raffinate purity increases from 79.1 to 87.2%. The second experiment presents the best performance results in terms of diethylacetal concentration at the raffinate stream ($C_{C,R}$ = 3.0 mol/L), productivity (PR = 4.65 kg L^{-1} day^{-1}) and desorbent consumption (DC = 7.45 L/kg). The acetaldehyde conversion is about 98% for all experiments. Higher desorbent flow rates will allow complete resin regeneration in section I and, consequently, the raffinate purity will increase. The acetaldehyde conversion is not 100%; in fact, the water adsorbed in the resin is not completely removed in section I and so it is carried by the resin entering section IV and is transported to section III, where it reacts with the diethylacetal to produce ethanol and acetaldehyde (opposite reaction). In fact, because of equipment limitations complete regeneration of the resin in zone I was not possible. Therefore, the use of a high desorbent flow rate leads to complete acetaldehyde conversion; unfortunately, the desorbent consumption increases.

The cyclic steady-state (CSS) concentration profiles ob-

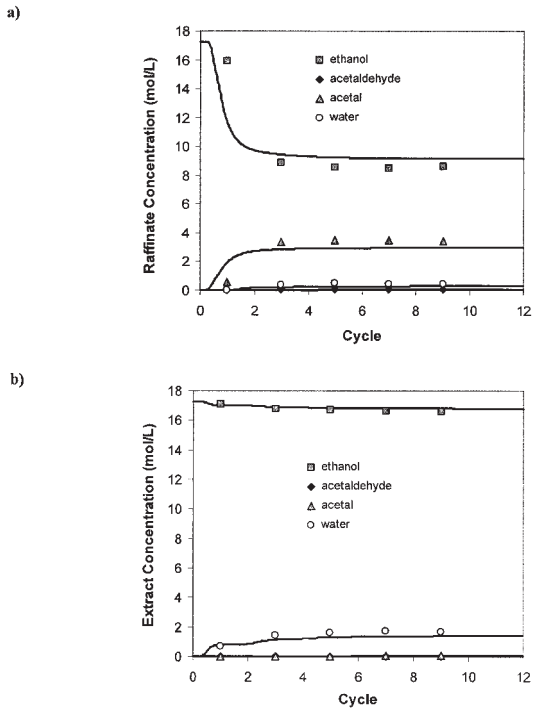

Figure 9. Experimental product concentrations collected for a whole cycle and calculated products concentration from the TMBR model, for run 2.

(a) Raffinate stream; (b) extract stream.

Table 9. Acetal Concentration in Raffinate and Water Concentration in Extract: Experimental and Predicted Values

Product Concentration	Acetal in Raffinate	Water in Extract
Experimental value at the middle of the switching time after 10 cycles	$C_{C,R}$ = 3.00 mol/L	$C_{D,X}$ = 1.65 mol/L
Experimental product concentrations collected for a whole cycle at the 9th cycle	$C_{C,R}$ = 3.44 mol/L	$C_{D,X}$ = 1.65 mol/L
Calculated product concentration at steady state from the TMBR model	$C_{C,R}$ = 2.99 mol/L	$C_{D,X}$ = 1.41 mol/L

tained experimentally at the middle of the switching time after 10 cycles are compared with the steady-state profiles simulated by the TMBR model in Figure 8. For all experiments, the reaction occurs in section III, and the acetaldehyde is completely consumed near the feed port. In section I, it is clear that the water is not completely desorbed from the resin, leading to a raffinate stream contamination with water. Figure 9 shows the experimental products concentration collected for a whole cycle at the 3rd, 5th, 7th, and 9th cycles and the extract and raffinate concentration histories as calculated from a TMBR model, for the second experiment. For both extract and raffinate, the amount of product is actually greater than that predicted. For sake of clarity, the experimental value at the middle of the switching time after 10 cycles, the concentration of experimental products collected for a whole cycle at the 9th cycle, and the concentration of calculated products at steady state from the TMBR model are presented in Table 9.

The experimental values of water concentration in the extract at the middle of the switching time and to the extract product collected for a whole cycle are equal, but slightly different from that predicted from the TMBR simulator. Most likely this is attributable to slight inaccuracies in the description of the highly favorable water adsorption isotherm and by the fact that the LDF approximation is used to describe the rate of adsorption.[49] However, for the amount of acetal in the raffinate the agreement between the experimental value at the middle of the switching time after 10 cycles and that calculated at steady state with the TMBR model is very good but different from the experimental acetal concentration in the raffinate collected for a whole cycle at the 9th cycle. Probably, the average cycle concentration calculated by the SMBR dynamic model could provide better results.

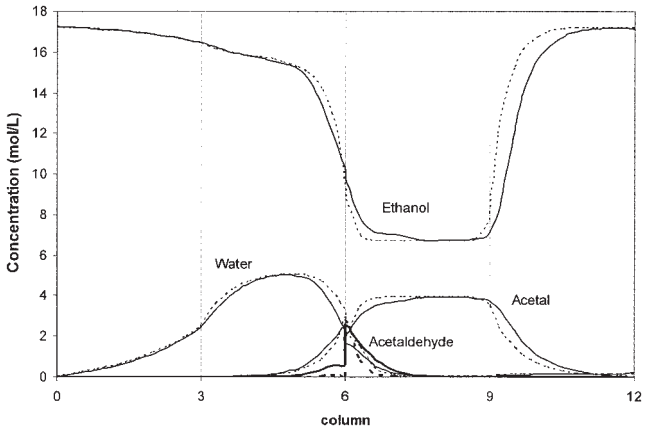

Figure 10. Comparison of the steady-state concentration profiles calculated with the TMBR model (dashed lines) and the concentration profiles at the middle of a switching time at cyclic steady state calculated with the SMBR model (solid lines), for the reference case.

Comparison of TMBR and SMBR models

A comparison of the steady-state concentration profiles calculated with the TMBR model and the CSS SMBR model in the middle of the switching time is presented in Figure 10. The operating conditions are presented in Table 10; the kinetic and adsorption parameters are those defined before. A slight difference between the equivalent TMBR and the real SMBR concentration profiles was observed around the feed and raffinate ports.

The SMBR performances were calculated (1) using the concentrations at the middle of the switching time and (2) using the averaged concentration over a switching time period, after reaching the cyclic steady state. There is a minor difference between the performance parameters predicted with the TMBR model and the CSS SMBR model using the averaged concentration over a switching time period (see Table 11).

The TMBR model describes well the experimental CSS SMBR internal concentration profiles at the middle of the switching time (see Figure 8) and well predicts the CSS SMBR performance calculated using the averaged species concentration over a switching time period. Therefore, the TMBR model was used to study the influence of the feed composition, switching time, and mass-transfer resistance onto the SMBR performance, in terms of minimum desorbent consumption and maximum productivity. The raffinate purity restriction was fixed at 95%: the extract purity is not so important because water is a secondary product.

Effect of feed composition

Ethanol is used both as desorbent and reactant; a high desorbent flow rate is necessary for complete regeneration of adsorbent in section I. In the reaction sections (II and/or III) the ethanol reacts with the acetaldehyde fed to the system. If the ethanol that enters the SMBR unit in the desorbent stream is enough to convert the acetaldehyde that is being introduced in the feed of pure acetaldehyde, this should lead to the best

Table 10. SMBR Operating Conditions for the Reference Case

Operating Conditions	
Q_D = 50.0 mL/min	$C_{A,F}$ = 8.57 mol/L
Q_F = 10 mL/min	$C_{B,F}$ = 8.96 mol/L
Q_R = 25 mL/min	
Q_X = 35 mL/min	L = 23 cm
Q_{rec} = 20 mL/min	d = 2.6 cm
t^* = 3.70 min	Configuration: 3–3–3–3

Table 11. Comparison of the SMBR Performance Calculated by TMBR and SMBR Models, for the Reference Case

Model	Performance Parameters				
	PUX (%)	*PUR* (%)	*PR* (kg L^{-1} day^{-1})	*DC* (L/kg)	*X* (%)
TMBR model (at the steady state)	99.9	97.8	17.1	4.27	99.7
SMBR model (averaged over the switching time)	99.7	98.0	17.2	4.24	99.7
SMBR model (at the middle of the switching time)	99.7	98.3	18.2	4.02	99.7

performance of the SMBR unit, given that for the same desorbent flow rate more acetal is being produced. However, the influence of feed composition on the acetal purity, acetaldehyde conversion, productivity, and ethanol consumption (Figure 11) shows that a feed containing 70–80 mol % of acetaldehyde leads to a better performance. For concentration of acetaldehyde $>$ 80% the conversion is $<$95% and thus the acetal purity decreases $<$95%.

A deeper understanding of the unit behavior is possible by analyzing the internal concentration profiles (Figure 12). The acetaldehyde internal profile is distributed in sections II and III, where the reaction occurs; sections I and IV play the same role as in a SMB system. For a molar fraction of acetaldehyde in the feed up to 80%, the reaction in section III is not complete and, consequently, the unreacted acetaldehyde goes to the raffinate stream leading to impure acetal. The reason for this behavior is that section II is characterized by a lack of ethanol and the reaction is chemical equilibrium controlled. Higher acetaldehyde concentrations will lead to higher excess of unreacted acetaldehyde and consequently the raffinate stream is contaminated. For feed systems with $<$70% of acetaldehyde, this species is completely consumed near the feed port and the SMBR unit operates like an SMB to separate acetal from water.

For each switching time, the ideal feed composition will depend on the desorbent flow rate (pure ethanol) and the feed that will be processed; acetaldehyde concentration should be high enough to increase the productivity without leading to a lack of ethanol in the reaction zone (II and III).

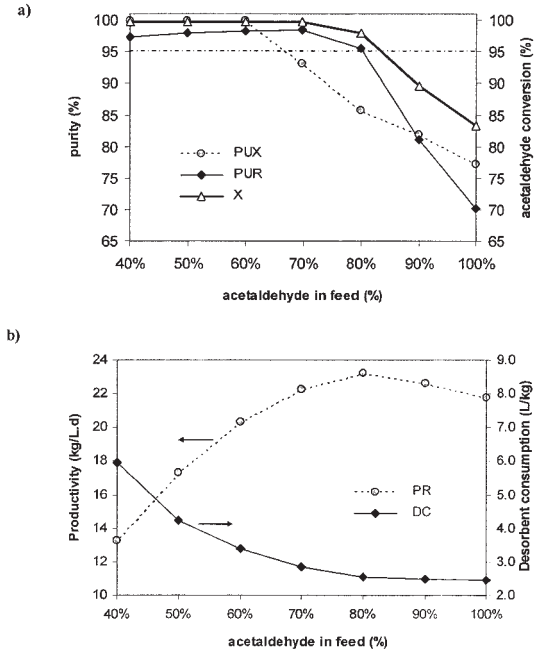

Figure 11. Effect of the feed composition [molar percentage (mol %) of acetaldehyde] in the performance parameters.

(a) Raffinate and extract purities and acetaldehyde conversion; (b) productivity and desorbent consumption.

Effect of switching time

The switching time sensitivity analysis was conducted for two situations:

(1) The feed is a 50% mixture of acetaldehyde (Figure 13): the acetaldehyde is completely consumed and appears only near the feed port, and the SMBR unit serves as an SMB unit.

(2) The feed is a 70% mixture of acetaldehyde (Figure 14): in this case, the acetaldehyde is not instantaneously consumed and sections II and III are used as reactive and separative zones.

For a 50% acetaldehyde feed composition the best performance achieved is a productivity of 17.3 kg L^{-1} day^{-1} and a desorbent consumption of 4.22 L/kg, for switching time range 3.7–4.1 min. The increase of acetaldehyde feed mole fraction up to 70% leads to a maximum productivity of 23.5 kg L^{-1} day^{-1} with a minimum desorbent consumption of 2.71 L/kg for a switching time of 3.9 min. In this case the switching time plays a fundamental role both for the reaction and the separation goals, as shown in Figure 14. Concentration profiles for ethanol, acetaldehyde, acetal, and water are detailed in Figure 15 for various switching times: 3.7, 3.9, and 4.1 min. Acetaldehyde is the middle adsorbed component when compared with ethanol and water. If the conditions of sections II and III guarantee the acetal/water separation, $t^* = 3.7$–4.1 min (Figure 15b), the switching time will affect the acetaldehyde net flow and acetaldehyde appears only in section II ($t^* = 3.7$ min) or in section III ($t^* = 4.1$ min) or in both sections ($t^* = 3.9$ min), and the residence time of acetaldehyde in those sections should be sufficient to achieve complete reaction. Considering the desired product acetal (Figure 15c) and for $t^* = 3.7$ min it is verified that some acetal is wasted in the extract stream ($C_{C,X} = 0.26$ mol/L), although the raffinate concentration is 4.60 mol/L. The reason for this is that the acetal produced at section II near the raffinate port does not have enough time to be desorbed and carried out with the liquid to section III. Increasing the switching time to 3.9 and 4.1 min, the extract concentration of acetal decreases to 0.01 and 0 mol/L, respectively. An analysis of the internal concentrations profiles of the byproduct water (Figure 15d) shows that water concentrations for the raffinate stream are 0.06, 0.04, and 0.33 mol/L, for switching times of 3.7, 3.9, and 4.1 min, respectively. When the

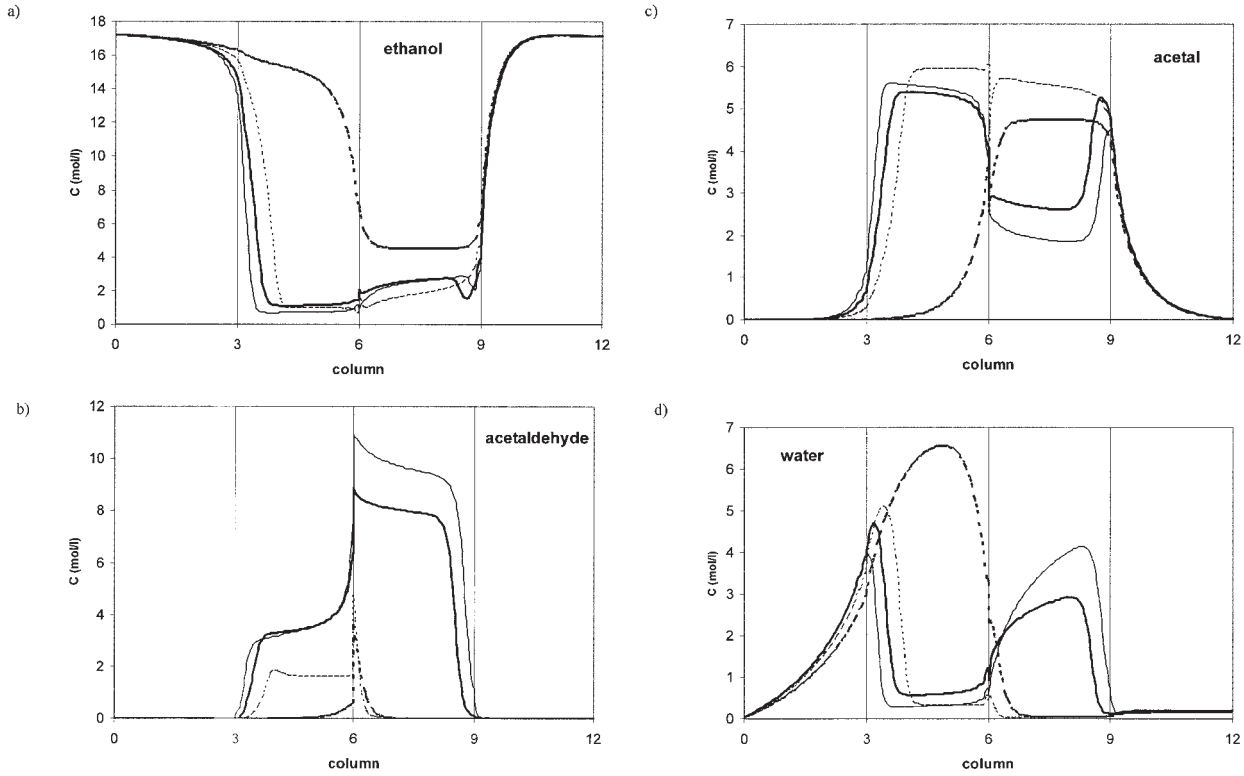

Figure 12. Effect of the feed composition (mol % of acetaldehyde) in the steady-state concentration profiles of ethanol, acetaldehyde, acetal, and water.

Legend: 100% (solid and thin line); 80% (solid and bold line); 70% (dashed and thin line); 60% (dashed and bold line).

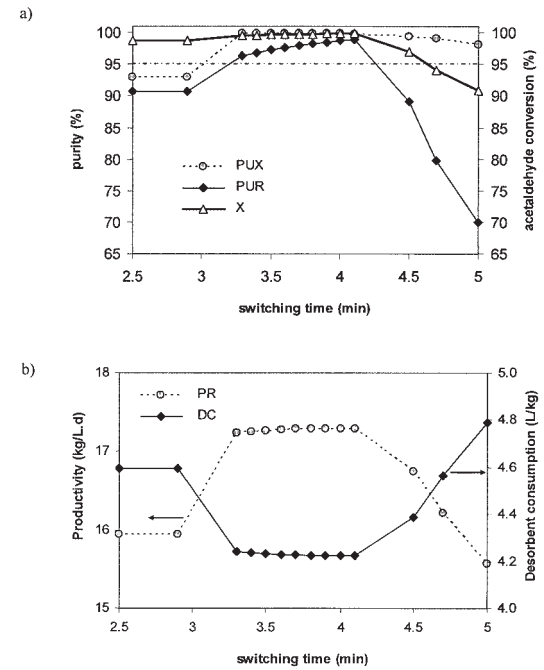

Figure 13. Effect of the switching time (51 mol % of acetaldehyde in feed) in the performance parameters.

(a) Raffinate and extract purities and acetaldehyde conversion; (b) productivity and desorbent consumption.

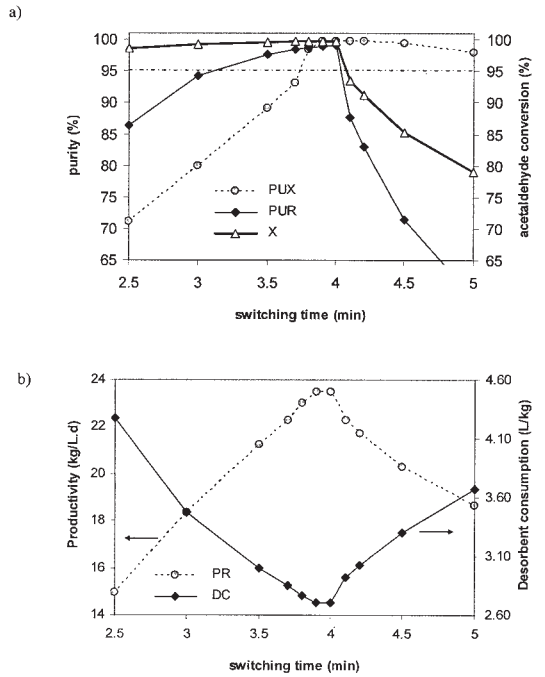

Figure 14. Effect of the switching time (70 mol % of acetaldehyde in feed) in the performance parameters.

(a) Raffinate and extract purities and acetaldehyde conversion; (b) productivity and desorbent consumption.

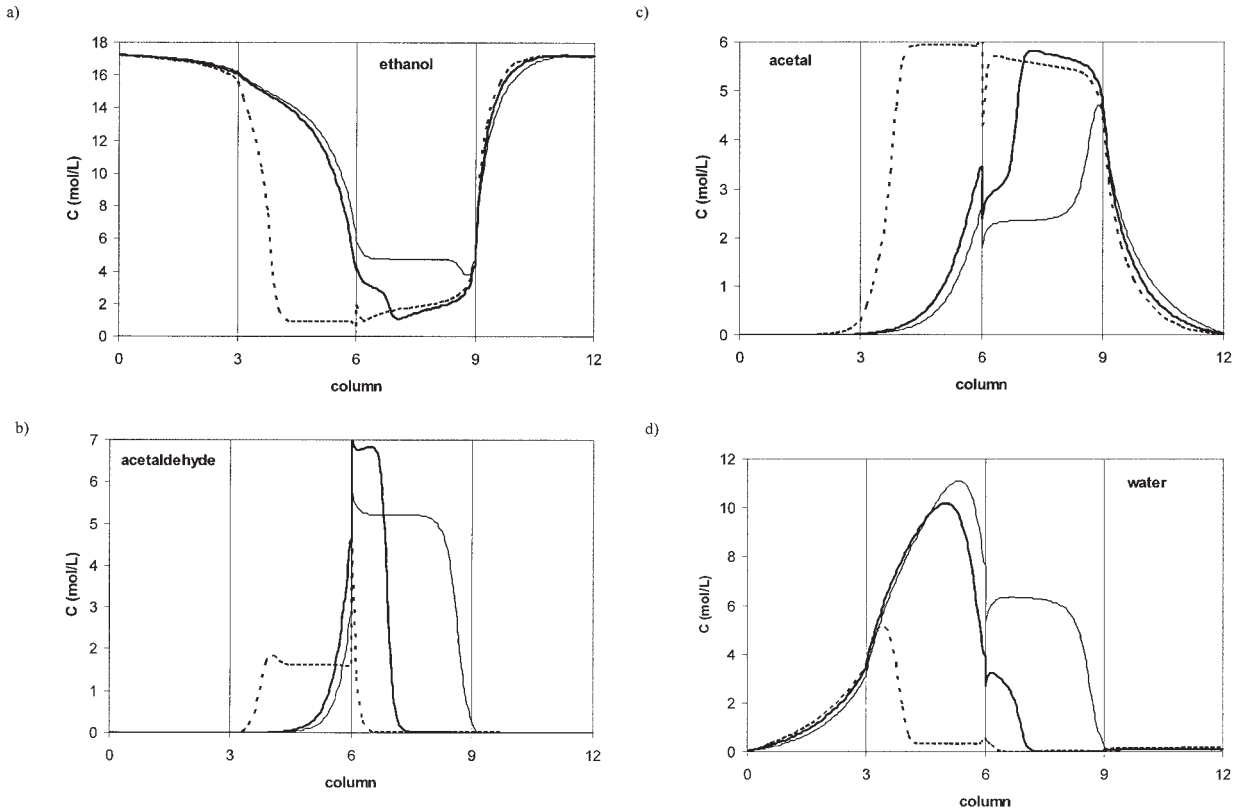

Figure 15. Steady-state concentration profiles of ethanol, acetaldehyde, acetal, and water for different switching times and for a 70 mol % of acetaldehyde in feed.

Legend: $t^* = 3.7$ min (dashed line); $t^* = 3.9$ min (solid line); $t^* = 4.1$ min (thin line).

reaction occurs in section III ($t^* = 4.1$ min), the water produced near the raffinate port contaminates the acetal stream. The best performance is obtained when the reaction occurs in both sections II and III ($t^* = 3.9$ min) because the resin is most efficiently used as catalyst. This is in agreement with the conclusion of Lode for the system of methyl acetate production.[34]

Effect of mass-transfer resistance

The mass-transfer resistances are critically important for the determination of the reaction/separation region that allows a given purity, mainly for a high degree of purity. For that reason, the sensitivity analysis of the global mass-transfer coefficient on the SMBR performance parameters is presented in Figure 16. The raffinate purity increases from 97.9% (reference case) to 99.5% by making the global mass-transfer coefficients calculated instantaneously and locally twice higher than at the reference case. If high acetal purity is an issue, the possibility of decreasing the particle size should be considered.

Reaction/separation region

The reaction/separation region defines the operation region where the product specifications are achieved (raffinate purity and acetaldehyde conversion $> 95\%$). The numerical procedure used to define the reaction/separation region consists of fixing at the same time the value of switching time and the values of fluid/solid interstitial velocity ratio ($\gamma_j = u_j/U_s$) in sections I and IV. These conditions are those from Table 10. By setting the γ_j values for sections I ($\gamma_I = 4.30$) and IV ($\gamma_{IV} = 0.515$) a region of reaction/separation is defined in a γ_{II}–γ_{III} plane.

The reaction/separation region is located within the region between the diagonal $\gamma_{II} = \gamma_{III}$, the horizontal line $\gamma_{III} = 0.515$, and γ_{III} axis. The diagonal $\gamma_{II} = \gamma_{III}$ corresponds to a zero feed flow rate, and thus γ_{III} must be higher than γ_{II}. The horizontal branch $\gamma_{III} = 0.515$ corresponds to a zero raffinate flow rate.

The algorithm for the construction of the reaction/separation region starts by setting a low value of the feed flow rate (0.02 mL/min) and the value of γ_{II} is 0.515. Then, the γ_{II} values were consecutively incremented by a steps of 0.001, sufficiently small to provide precise determination of the reaction/separation region. For each γ_{II}, the value of γ_{III} was calculated from the mass balance in the feed node. The purities of extract and raffinate were calculated for each pair of (γ_{II}, γ_{III}). The values that guarantee the minimum 95% purity in both extract and raffinate were selected to build the reaction/separation region. At the end of this cycle, the line of reaction/separation corresponding to the feed flow rate is defined and then the feed flow rate is increased to a higher value. The simulation procedure ends with the last value of the maximum feed flow rate, which gives extract and raffinate purities of 95% (vertex of the reaction/separation region). Above that feed flow rate value the purity requirement cannot be fulfilled for any pair of values of (γ_{II}, γ_{III}).

Figure 17 shows two reaction/separation regions for 95%

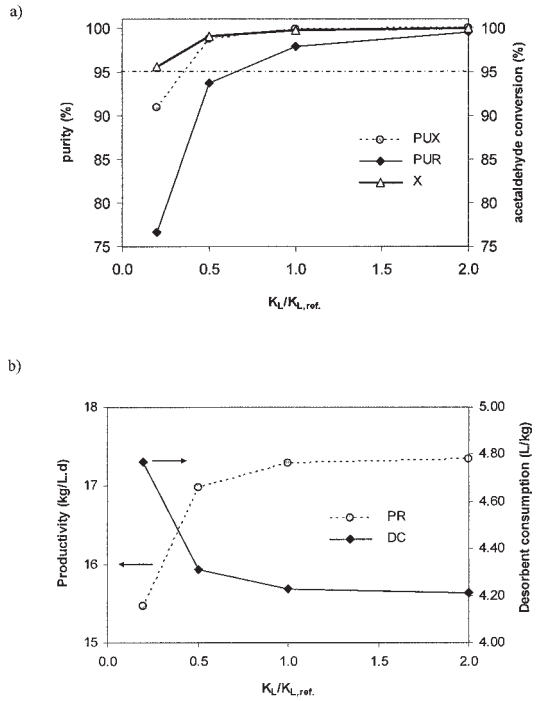

Figure 16. Sensitivity analysis to mass transfer resistance (51 mol % of acetaldehyde in feed, t^* = 3.7 min) in the performance parameters.

(a) Raffinate and extract purities and acetaldehyde conversion; (b) productivity and desorbent consumption.

purity criteria: (1) calculated by the TMBR model; (2) calculated by the SMBR model. The two regions are very similar in shape and size, although a small deviation occurs, mainly from the border of impure raffinate. The vertices calculated with the TMBR model (gray symbol) and with the SMBR model (black symbol) have close values, meaning that the optimal operating conditions calculated from the SMBR and TMBR models have comparable performances. The reaction/separation region obtained with the SMBR model is the smaller one because the

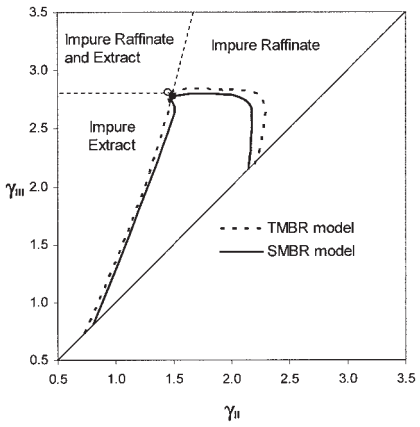

Figure 17. Reaction/separation regions calculated with the TMBR (solid line: γ_I = 4.30; γ_{IV} = 0.515) and the SMBR (dashed line: γ_I^* = 5.30; γ_{IV}^* = 1.52) models.

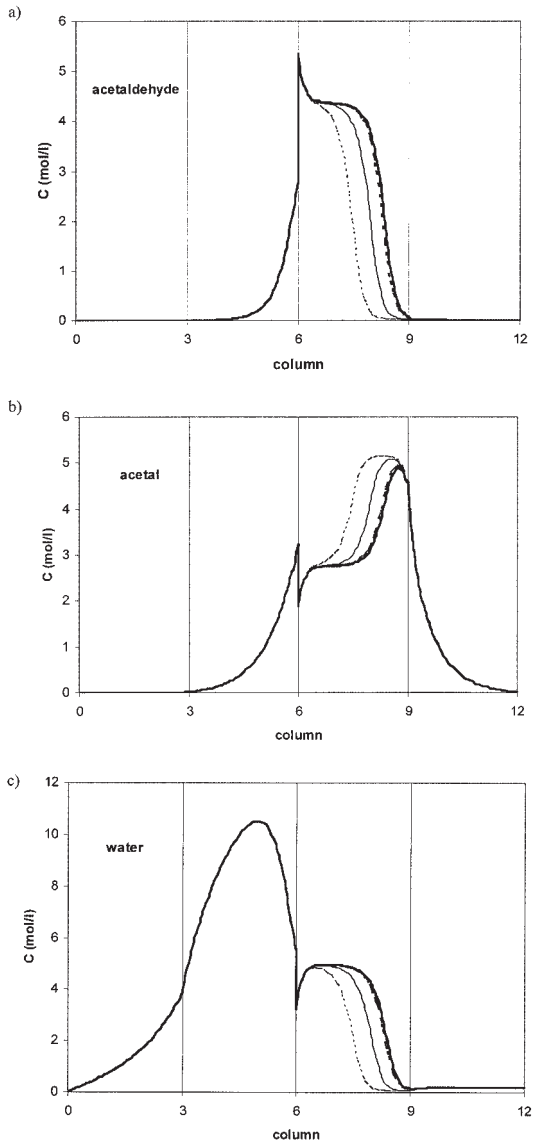

Figure 18. Time evolution of the concentration profiles of acetaldehyde, acetal, and water.

γ_I = 4.302; γ_{II} = 1.632; γ_{III} = 2.844; γ_{IV} = 0.515. Legend: t = 400 min (dashed and thin line); t = 600 min (solid and thin line); t = 800 min (dashed and bold line); t = 1000 min (solid and bold line).

residence time in section III of the SMBR unit is lower than that in the TMBR unit. In fact, the liquid velocities are higher in the SMBR unit; therefore the acetaldehyde conversion is smaller and the unreacted acetaldehyde will contaminate the raffinate stream, a phenomenon first noticed by Lode.[50] Both reaction/separation regions present a plateau at about γ_{III} = 2.82 and 2.78 for the TMBR and SMBR models, respectively. This is attributed to the reactive front containing acetaldehyde and water traveling along section III, as in the fixed-bed reactor,[45] and reaching the raffinate port thus contaminating the raffinate stream (see Figure 18). The reaction occurs until complete consumption of acetaldehyde because ethanol is in great excess, with respect to acetaldehyde, and water displaces acetal from the stationary phase. In this reaction front, the

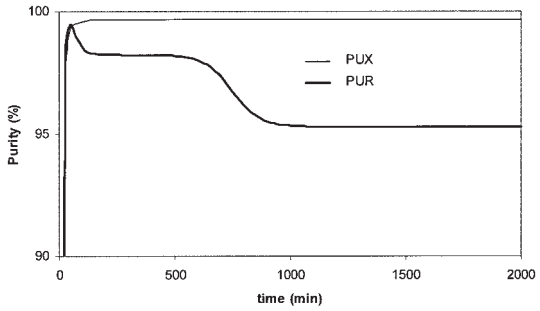

Figure 19. Time evolution of purities of extract and raffinate.

$\gamma_I = 4.302$; $\gamma_{II} = 1.632$; $\gamma_{III} = 2.844$; $\gamma_{IV} = 0.515$.

acetaldehyde front concentration exhibits a constant pattern behavior because it propagates along the column without changing its shape (Figure 18a). Because water is being preferentially adsorbed by the resin while it is produced, the velocity of the water front is lower than that of the acetaldehyde front (Figure 18c). The water front also exhibits a constant pattern behavior. The acetal produced is immediately desorbed and collected at the raffinate port (Figure 18b).

The movement of the reaction front is observed in the raffinate purity history (Figure 19). At the beginning of the SMBR operation the acetal produced is separated from the reactive zone and reaches the raffinate port (purity increases). At the same time the water that is produced is strongly adsorbed by the resin and carried out with the solid phase to zone IV, slightly decreasing the raffinate purity. After that, it was expected that after 10 cycles (444 min), given that both purities remain constant, that the steady state was achieved. Only by analysis of the time evolution of the internal concentration profiles was it possible to observe a reactive front moving along section III, whereupon its arrival at the raffinate port did the purity decrease again.

The above studies concerning the effect of the feed composition and the switching time were carried out considering the individual effect of each variable while keeping the others constant. Obviously, to obtain the best SMBR unit performance a full optimization for different switching times, feed composition, and SMBR flow rates has to be done. Thus, for a given feed concentration, the fluid/solid interstitial velocity ratio should be optimized. The optimal operating point corresponds to the vertex of the reaction/separation region, where the maximum feed flow rate can be processed in the SMBR unit.

The influence of the feed composition on the reaction/separation region calculated with the TMBR model is shown in Figure 20, for $\gamma_I = 4.30$ and $\gamma_{IV} = 0.515$, and for three different feed molar fractions of acetaldehyde (1, 51, and 100%). The vertices of these regions are indicated with black circles. The operating region for 1% feed molar fraction of acetaldehyde corresponds to the limiting case of a SMB unit to separate acetal from water, given that acetaldehyde is in a very small amount relative to ethanol and is thus instantaneously consumed near the feed port. This region (95% purity) exhibits the shape of a linear system in the presence of mass-transfer resistances; because ethanol is in great excess the competitive isotherms of acetaldehyde, acetal, and water approach the linear behavior. By increasing the acetaldehyde content, the

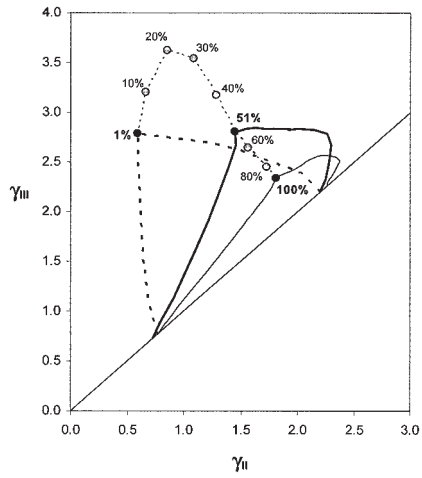

Figure 20. Reaction/separation regions calculated with the TMBR model for acetaldehyde feed concentration of 1% (dashed line), 51% (bold line), and 100% (thin line) and optimal operating points for feed molar fractions of acetaldehyde of 1, 10, 20, 30, 40, 51, 60, 80, and 100%.

$\gamma_I = 4.30$; $\gamma_{IV} = 0.515$.

border of the operating region becomes increasingly more distorted. The effect of the feed concentration onto the qualitative shape of the reaction/separation region was studied for the system of methyl acetate production, considering the equilibrium theory model for the SMBR with infinitely fast reaction rate (instantaneous reaction equilibrium).[51]

In Figure 20 the optimal operating points (the vertices of the reaction/separation regions) for the other six different feed molar fractions of acetaldehyde (10, 20, 30, 40, 60, and 80%) are indicated with gray circles. By increasing the distance from the diagonal of the γ_{II}–γ_{III} plane, the feed flow rate is increased. Therefore, the SMBR unit can process a maximum feed flow rate when using an acetaldehyde content of about 20%. For higher values of acetaldehyde molar fraction the maximum feed processed decreases continuously by increasing the feed acetaldehyde content. Figure 21 shows the raffinate productivity, desorbent consumption, and concentration of ac-

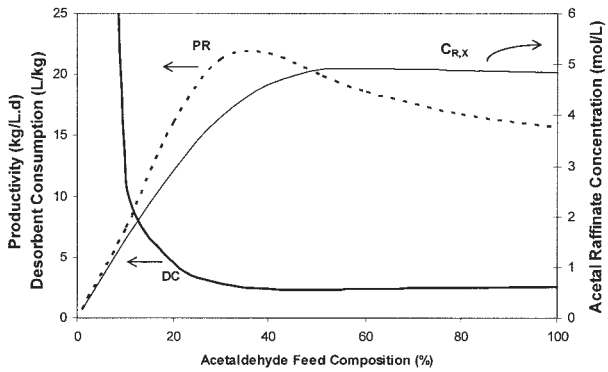

Figure 21. SMBR performance for the optimal operating points shown in Figure 20 as a function of the acetaldehyde feed composition.

etal at the raffinate stream as a function of the feed molar fraction of acetaldehyde, for the optimal operating points. The SMBR unit productivity reaches a maximum of 22 kg_{acetal} $L^{-1}_{adsorbent}$ $day^{-}1$ at 30% of acetaldehyde molar fraction and then decreases continuously with acetaldehyde content increment. The desorbent consumption has a lower value of 2.3 $L_{ethanol}$/kg_{acetal} at 40% of acetaldehyde molar fraction and then remains constant. The maximum value of 4.92 mol/L acetal raffinate concentration is achieved at a feed composition of acetaldehyde of 50%. This analysis was obtained for fixed flow rates in sections I and IV. The influence of these parameters on the SMBR unit performance should also be taken in consideration in further optimization of the SMBR process.

Conclusions

Diethylacetal was produced from the liquid-phase reversible reaction between ethanol and acetaldehyde, using Amberlyst® 15 as catalyst and selective adsorbent, in a simulated moving-bed reactor. The methodology used combines modeling/simulation with laboratory- and pilot-scale experiments. The kinetic law of the reaction was measured from experiments in a batch catalytic reactor. The adsorption parameters were obtained from experiments performed in a fixed-bed adsorption column. Laboratory experiments in fixed-bed adsorptive reactors were performed and used to validate model and simulation tools. Experimentally, the best performance obtained in an SMBR was a raffinate purity of 87%, and the acetaldehyde conversion about 98%, a diethylacetal concentration at the raffinate stream of 3.0 mol/L, and 4.65 kg_{acetal} $L^{-1}_{adsorbent}$ day^{-1} and 7.45 $L_{ethanol}$/kg_{acetal} for productivity and desorbent consumption, respectively. A patent concerning the SMBR technology for acetals production has already been granted.[52] Simulations show that high diethylacetal purity and complete acetaldehyde conversion are obtained by increasing the desorbent flow rate. For example, when an SMBR unit with 12 columns (configuration: 3–3–3–3) is operated with Q_D = 50 mL/min, Q_F = 10 mL/min (70% of acetaldehyde), Q_R = 25 mL/min, Q_X = 35 mL/min, and t^* = 3.9 min, diethylacetal with 99% purity is obtained and acetaldehyde is 99.8% converted. The SMBR unit productivity is 23.5 kg_{acetal} $L^{-1}_{adsorbent}$ day^{-1} and the desorbent consumption is 2.71 $L_{ethanol}$/kg_{acetal}.

Acknowledgments

We gratefully acknowledge the financial support of FCT (Fundação para a Ciência e Tecnologia, Portugal) Project Grant POCTI/EQU/40695/2001 and the award from Solvay Ideas Challenge (2003) for this work.

Notation

a = liquid-phase activity, dimensionless
C = liquid-phase concentration, mol/m^3
$\bar{C}_p$ = average liquid-phase concentration inside the particle, mol/m^3
d_p = particle diameter, m
D_{ax} = axial dispersion, m^2/s
DC = desorbent consumption, $L_{ethanol}$ $kg^{-1}_{catalyst}$
K = Langmuir equilibrium parameter, m^3/mol
K_L = global mass-transfer coefficient, m/s
k_C = kinetic constant, mol $kg^{-1}_{catalyst}$ s^{-1}
K_D = adsorption constant for Eq. 4, dimensionless
K_{eq} = equilibrium constant, dimensionless
L = section length, m
L_c = column length, m
Pe = Peclet number
PR = raffinate productivity, kg_{acetal} $L^{-1}_{adsorbent}$ day^{-1}
PUR = raffinate purity, %
PUX = extract purity, %
q = solid phase concentration, $mol/m^3_{adsorbent}$
Q_{ads} = adsorption capacity, $mol/m^3_{adsorbent}$
Q = volumetric flow rate, m^3/s
$\Re$ = reaction rate, mol $kg^{-1}_{catalyst}$ s^{-1}
r_p = particle radius, m
t = time coordinate, s
t^* = switching time, min
T = temperature, K
u = interstitial fluid velocity, m/s
U_s = interstitial solid velocity, m/s
V_{ml} = molar volume in the liquid phase, m^3/mol
X = acetaldehyde conversion, %
z = axial coordinate, m

Greek letters

ε = bulk porosity, dimensionless
ε_p = particle porosity, dimensionless
ν = stoichiometric coefficient, dimensionless
γ = ratio between the TMBR liquid and solid interstitial velocities, dimensionless
γ^* = ratio between the SMBR liquid and solid interstitial velocities, dimensionless
η = effectiveness factor of the catalyst, dimensionless
ρ_b = bulk density, kg/m^3
ρ_p = particle density, kg/m^3

Subscripts

D = relative to the desorbent
F = relative to the feed
i = relative to component i (i = A, B, C, D)
j = relative to section j (i = I, II, III, IV)
R = relative to the raffinate
X = relative to the extract
0 = relative to initial conditions

Literature Cited

1. Boennhoff K. *1,1-Diethoxyethane as Diesel Fuel*. DE Patent No. 2,911,411; 1980.
2. Boennhoff K. *Method for Enhancing the Ignition Performance of Dialkoxyalkanes Used as Diesel Fuel, in Particular 1,1-Diethoxyethane*. DE Patent No. 3,136,030; 1983.
3. Golubkov A, Golubkov I. *Motor Fuel for Diesel, Gas-Turbine and Turbojet Engines*. U.S. Patent No. 02/0026744 A1; 2002.
4. Laborde MA. *Producción de Acetal a Partir de Bioetanol*. Buenos Aires, Argentina: Ediciones CYTED; 2003.
5. Bramwyche PL, Mudgan M, Stanley HM. *Manufacture of Diethyl Acetal*. U.S. Patent No. 2 519 540; 1950.
6. Petersen ML. *Process for the Production of Liquid Acetals*. U.S. Patent No. 4 024 159; 1977.
7. Kohlpaintner C, Schulte M, Falbe J, Lappe P, Weber J. Aldehydes, aliphatic and araliphatic. *Ullmann's Encyclopedia of Industrial Chemistry*. Weinheim, Germany: Wiley-VCH; 1999.
8. Morrison R, Boyd R. *Organic Chemistry*. 4th Edition. London: Allyn & Bacon; 1983.
9. Mazzotti M, Kruglov A, Neri B, Gelosa D, Morbidelli M. A continuous chromatographic reactor: SMBR. *Chem Eng Sci.* 1996;51:1827-1836.
10. Mazzotti M, Neri B, Gelosa D, Kruglov A, Morbidelli M. Kinetics of liquid-phase esterification catalyzed by acidic resins. *Ind Eng Chem Res.* 1997;36:3-10.
11. Backaus AA. *Continuous Process for the Manufacture of Esters*. U.S. Patent No. 1 400 849; 1921.
12. Agreda VH, Partin LR. *Reactive Distillation Process for the Production of Methyl Acetate*. U.S. Patent No. 4 435 595; 1984.
13. Sneesby MG, Tadé MO, Smith TN. Multiplicity and pseudo-multiolicity in MTBE and ETBE reactive distillation. *Trans IChemE*. 1998; 76A:525-531.

14. Sundmacher K, Uhde G, Hoffmann U. Multiple reactions in catalytic distillation processes for the production of the fuel oxygenates MTBE and TAME: Analysis by rigorous model and experimental validation. *Chem Eng Sci.* 1999;54:2839-2847.
15. Oudshoorn OL, Janissen M, van Kooten WEJ, van Bekkum H, van den Bleek CM, Calis HPA. A novel structured catalyst packing for catalytic distillation of ETBE. *Chem Eng Sci.* 1999;54:1413-1418.
16. Oost C, Hoffmann U. The synthesis of tertiary amyl methyl ether (TAME): Microkinetics of the reactions. *Chem Eng Sci.* 1996;51:329-340.
17. Kolah AK, Mahajani SM, Sharma MM. Acetalization of formaldehyde with methanol in batch and continuous reactive distillation. *Ind Eng Chem Res.* 1996;35:3707-3720.
18. Hasanoglu A, Salt Y, Keleser S, Ozkan S, Dincer S. Pervaporation separation of ethyl acetate–ethanol binar mixtures using polydimethylsiloxane membranes. *Chem Eng Prog.* 2005;44:375-381.
19. Smitha B, Suhanya D, Sridhar S, Ramakrishna M. Separation of organic–organic mixtures by pervaporation—A review. *J Membr Sci.* 2004;241:1-21.
20. Ball IJ, Huang S-C, Wolf RA, Shimano JY, Kaner RB. Pervaporation studies with polyaniline membranes and blends. *J Membr Sci* 2000; 174:161-176.
21. AW Verkerk, P van Male, MAG Vorstman, Keurentjes JTF. Properties of high flux ceramic pervaporation membranes for dehydration of alcohol/water mixtures. *Sep Purif Technol.* 2001;22–23:689-695.
22. Ray AK, Carr RW, Aris R. The simulated countercurrent moving bed chromatographic reactor: A novel reactor–separator. *Chem Eng Sci.* 1994;49:469-480.
23. Tonkovich ALY, Carr RW. A simulated countercurrent moving-bed chromatographic reactor for the oxidative coupling of methane: Experimental results. *Chem Eng Sci.* 1994;49:4647-4656.
24. Hashimoto K, Adachi S, Noujima H, Ueda Y. A new process combining adsorption and enzyme reaction for producing higher-fructose syrup. *Biotechnol Bioeng.* 1983;25:2371-2393.
25. Silva EB, Souza AAU, Souza SGU, Rodrigues AE. Simulated moving bed technology in the reactive process of glucose isomerization. *Adsorption*. 2005;11:847-851.
26. Zhang Z, Hidajat K, Ray AK. Optimal design and operation of SMB reactor: Production of high fructose syrup by isomerization of glucose. *Biochem Eng J.* 2004;21:111-121.
27. Toumi A, Engell S. Optimization-based control of a reactive SMB process for glucose isomerization. *Chem Eng Sci.* 2004;59:3777-3792.
28. Meurer M, Altenhöner U, Strube J, Untiedt A, Schmidt-Traub H. Dynamic simulation of a simulated-moving-bed chromatographic reactor for the inversion of sucrose. *Starch.* 1996;48:452-457.
29. Azevedo DCS, Rodrigues AE. Design methodology and operation of a simulated moving bed reactor for the inversion of sucrose and glucose-fructose separation. *Chem Eng J.* 2001;82:95-107.
30. Kawase M, Pilgrim A, Araki T, Hashimoto K. Lactosucrose production using simulated moving-bed reactor. *Chem Eng Sci.* 2001;51: 2971-2976.
31. Kawase M, Suzuki TB, Inoue K, Yoshimoto K, Hashimoto K. Increased esterification conversion by application of the simulated moving-bed reactor. *Chem Eng Sci.* 1996;51:2971-2976.
32. Migliorini C, Fillinger M, Mazzotti M, Morbidelli M. Analysis of simulated moving-bed reactors. *Chem Eng Sci.* 1999;54:2475-2480.
33. Kawase M, Inoue Y, Araki T, Hashimoto K. The simulated moving-bed reactor for production of bisphenol A. *Catal Today.* 1999;48:1-4.
34. Lode F, Houmard M, Migliorini C, Mazzotti M, Morbidelli M. Continuous reactive chromatography. *Chem Eng Sci.* 2001;56:269-291.
35. Zhang Z, Hidajat K, Ray AK. Application of simulated countercurrent moving-bed chromatographic reactor for MTBE synthesis. *Ind Eng Chem Res.* 2001;40:5305-5316.
36. Hotier G, Dulot H, Bailly M, Ragil K. *Simultaneous Process for Simulated Moving Bed Dismutation and Separation of Toluene into Benzene and Xylenes*. U.S. Patent No. 6 429 346 B2; 2002.
37. Fricke J, Meurer M, Dreisörner J, Schmidt-Traub H. Effect of process parameters on the performance of a simulated moving bed reactor chromatographic reactor. *Chem Eng Sci.* 1999a;54:1487-1492.
38. Fricke J, Meurer M, Schmidt-Traub H. Design and layout of simulated-moving-bed chromatographic reactors. *Chem Eng Technol.* 1999b; 22:835-839.
39. Dünnebier G, Fricke J, Klatt K-U. Optimal design and operation of simulated moving bed chromatographic reactors. *Ind Eng Chem Res.* 2000;39:2290-2304.
40. Fricke J, Schmidt-Traub H. A new method supporting the design of simulated moving bed chroamtographic reactors. *Chem Eng Process.* 2003;42:237-248.
41. Zhang Z, Hidajat K, Ray AK. Multiobjective optimization of simulated countercurrent moving bed chromatographic reactor (SCMCR) for MTBE synthesis. *Ind Eng Chem Res.* 2002;41:3213-3232.
42. Silva VMTM, Rodrigues AE. Synthesis of diethylacetal: Thermodynamic and kinetic studies. *Chem Eng Sci.* 2001;56:1255-1263.
43. Silva VMTM. *Diethylacetal Synthesis in Simulated Moving Bed Reactor*. PhD Thesis. Porto, Portugal: University of Porto; 2003.
44. Fredeslund A, Gmehling J, Rasmussen P. *Vapor–Liquid Equilibria Using UNIFAC*. Amsterdam: Elsevier; 1977.
45. Silva VMTM, Rodrigues AE. Diethylacetal synthesis with acid resin catalysts: Dynamics of a fixed bed adsorptive reactor. *AIChE J.* 2002; 48:625-634.
46. Glueckauf E. Theory of chromatography. Part 10. Formulae for diffusion into spheres and their application to chromatography. *Trans Faraday Soc.* 1955;51:1540-1551.
47. Ruthven DM. *Principles of Adsorption and Adsorption Processes.* 1st Edition. New York, NY: Wiley; 1984.
48. gPROMS. *gPROMS v2.2.3 User Guide.* London: Process System Enterprise Ltd.; 2003.
49. Meissner JP, Carta G. Continuous regioselective enzimatic esterification in a simulated moving bed reactor. *Ind Eng Chem Res.* 2002;41: 4722-4732.
50. Lode F, Mazzotti M, Morbidelli M. Comparing true countercurrent and simulated moving-bed chromatographic reactors. *AIChE J.* 2003; 49:977-990.
51. Ströhlein G, Mazzotti M, Morbidelli M. Optimal operation of simulated-moving-bed reactors for nonlinear adsorption isotherms and equilibrium reactions. *Chem Eng Sci.* 2005;60:1525-1533.
52. Silva VMTM, Rodrigues AE. *Processo Industrial de Produção de Acetais num Reactor Adsorptivo de Leito Móvel Simulado*. PT Patent No. 103,123 (pending); 2004.
53. Reid RC, Prausnitz JM, Poling BE. *The Properties of Gases and Liquids*. 4th Edition. New York, NY: McGraw-Hill; 1987.
54. Fredeslund A, Jones RM, Prausnitz JM. Supplement to program UNIFAC. Group-contribution estimation of activity coefficients in nonideal liquid mixtures (personal communication). Berkeley, CA: Dept. of Chemical Engineering, University of California; 1998.
55. Cristófoli FF, Espinosa J, Aguirre PA. Design and synthesis of acetal separation and purification process. Proc of ENPROMER'99—II Congresso de Engenharia de Processos do MERCOSUL, Florianópolis, Santa Catarina, Brazil; 1999.

Manuscript received Oct. 19, 2004, and revision received Feb. 15, 2005.